Journal of Solid State Chemistry **161,** 57–62 (2001)
doi:10.1006/jssc.2001.9266, available online at http://www.idealibrary.com on IDEAL®

$SbSb_xM_{1-x}O_4$ ($M = Nb^V$ or Ta^V): Solid Solution Behavior and Second-Harmonic Generating Properties

Kang Min Ok, N. S. P. Bhuvanesh, and P. Shiv Halasyamani[1]

Department of Chemistry, University of Houston, 4800 Calhoun Boulevard, Houston, Texas 77204-5003

Received February 26, 2001; in revised form May 24, 2001; accepted June 7, 2001; published online August 22, 2001

The solid solution behavior and second-harmonic generating (SHG) properties of $SbSb_xM_{1-x}O_4$ ($M = Nb^V$ or Ta^V) ($x = 0.0$, 0.2, 0.4, 0.5, 0.6, 0.8, and 1.0) have been investigated by powder X-ray diffraction and nonlinear optical (NLO) measurements. Both $SbNbO_4$ and $SbTaO_4$ form solid solutions with α-Sb_2O_4. All the materials crystallize in the non-centrosymmetric space group $Pna2_1$, with $Sb^{III}O_4E$ polyhedra linked to M^VO_6 ($M^V = Sb^V$, Nb^V, or Ta^V) octahedra. SHG data is presented for the solid solutions and α-Sb_2O_4, $SbNbO_4$, and $SbTaO_4$. With respect to the $SbSb_xM_{1-x}O_4$ phases, NLO measurements indicate a substantial decrease in SHG efficiency for $x \geq 0.6$. This decrease is attributable to the "nonpolar" nature of the Sb^VO_6 octahedra compared with the "polar" nature of Nb^VO_6 or Ta^VO_6.

Key Words: **oxides; solid solution; second-harmonic generation; powder X-ray diffraction.**

INTRODUCTION

The elucidation of structure–property relationships remains an ongoing challenge in solid-state materials chemistry. This is particularly true for second-order nonlinear optical (NLO), i.e., second-harmonic generating (SHG), materials (1–5). Viable SHG materials should possess the following attributes: chemical stability, transparency in the relevant wavelengths, and the ability to withstand laser irradiation, but most importantly the material must be crystallographically non-centrosymmetric (NCS) (6). In a review of NCS oxides (3), we determined the influence of a second-order Jahn–Teller (SOJT) distortion (7–13) on the acentric structure. In addition, we recently reported the syntheses, structures, and SHG behavior of some compounds that contain SOJT distorted cations (14–16). Through the powder SHG measurements we were able to estimate $\langle d_{ijk}^{2\omega} \rangle$, the *average* NLO bond susceptibility. One of the aims of our research is not only to synthesize SHG materials but also to understand the structural origin of the NLO phenomenon. With this in mind, we investigated the α-Sb_2O_4 (17, 18), $SbNbO_4$, and $SbTaO_4$ (19, 20) oxides. These compounds represent an isostructural oxide series, crystallizing in the NCS space group $Pna2_1$. The materials consist of $Sb^{III}O_4E$ polyhedra, where E is the nonbonded electron pair, and MO_6 octahedra ($M = Sb^V$, Nb^V, or Ta^V). With respect to connectivity, the structures can be described as $[SbO_{4/3}]^{1/3+}$ cations linked to $[MO_{4/2}O_{2/3}]^{1/3-}$ anions. A representation of the structure is given in Fig. 1. Both $SbNbO_4$ and $SbTaO_4$ are SHG active and ferroelectric with Curie temperatures of 605 and 600°C, respectively (21). The solid solution behavior of α-Sb_2O_4–$SbNbO_4$ and α-Sb_2O_4–$SbTaO_4$ has been briefly discussed (22), but a detailed study was not carried out. In this paper we describe the synthesis and SHG behavior of the $SbSb_xNb_{1-x}O_4$ and $SbSb_xTa_{1-x}O_4$ solid solutions. In addition, we describe in detail the SHG behavior of α-Sb_2O_4, $SbNbO_4$, and $SbTaO_4$, including an estimate of a specific NLO bond susceptibility tensor, d_{333}, for $SbNbO_4$ and $SbTaO_4$.

EXPERIMENTAL

Synthesis. The $SbSb_xM_{1-x}O_4$ (M = Nb or Ta; $x = 0.2$, 0.4, 0.5, 0.6, 0.8) phases were synthesized through standard solid-state techniques. Stoichiometric amounts of Sb_2O_3 (Alfa, 99.6%) with either Nb_2O_5 (Aldrich, 99.99%) or Ta_2O_5 (Aldrich, 99%) and Sb_2O_5 (Aldrich, 99.995%) were thoroughly ground with an agate mortar and pestle and pressed into pellets. The pellets were wrapped with platinum foil and introduced into a quartz tube that was sealed under vacuum. Each tube was heated to 550°C for 3 h and then to 650°C (800°C for $SbSb_xTa_{1-x}O_4$ phases) for 48 h. The samples were cooled at a rate of 10°C/min to room temperature. Polycrystalline α-Sb_2O_4 was synthesized by heating Sb_2O_3 in air at 600°C for 24 h. $SbNbO_4$ and $SbTaO_4$ were prepared as previously reported (23, 24).

Diffraction and crystal structure refinement. The X-ray powder diffraction data were collected on a Scintag

[1] To whom correspondence should be addressed. Fax: 713-743-2787. E-mail: psh@uh.edu.

0022-4596/01 $35.00

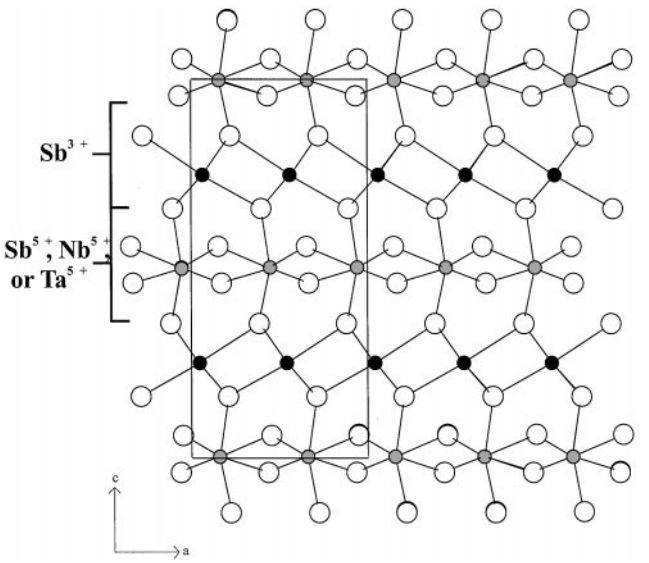

FIG. 1. Ball-and-stick representation of $SbMO_4$ ($M = Sb^V$, Nb^V, or Ta^V).

TABLE 1
Unit Cell Constants for $Sb(Sb_xM_{1-x})O_4$ (M = Nb or Ta)

Compound	a (Å)	b (Å)	c (Å)	V (Å^3)
$SbNbO_4$	5.5630(3)	4.9305(3)	11.8038(6)	323.76(3)
$Sb(Sb_{0.2}Nb_{0.8})O_4$	5.5458(2)	4.9095(1)	11.8009(3)	321.30(4)
$Sb(Sb_{0.4}Nb_{0.6})O_4$	5·5241(2)	4.8866(2)	11.7982(5)	318.48(5)
$Sb(Sb_{0.5}Nb_{0.5})O_4$	5.5140(2)	4.8761(2)	11.7961(5)	317.16(5)
$Sb(Sb_{0.6}Nb_{0.4})O_4$	5.4982(2)	4.8638(2)	11.7916(5)	315.33(5)
$Sb(Sb_{0.8}Nb_{0.2})O_4$	5·4733(4)	4·8433(3)	11.7927(8)	312.61(7)
α-Sb_2O_4	5.4429(3)	4.8084(3)	11.7810(6)	308.33(3)
Compound	a (Å)	b (Å)	c (Å)	V (Å^3)
$SbTaO_4$	5.5361(9)	4.9117(3)	11.8215(6)	321.45(4)
$Sb(Sb_{0.2}Ta_{0.8})O_4$	5.5258(1)	4.9004(1)	11.8125(3)	319.87(4)
$Sb(Sb_{0.4}Ta_{0.6})O_4$	5.5090(1)	4.8836(1)	11.8057(3)	317.62(4)
$Sb(Sb_{0.5}Ta_{0.5})O_4$	5.5019(2)	4.8762(2)	11.8038(4)	316.68(5)
$Sb(Sb_{0.6}Ta_{0.4})O_4$	5.4922(2)	4.8646(2)	11.7988(4)	315.23(5)
$Sb(Sb_{0.8}Ta_{0.2})O_4$	5.4680(2)	4.8380(2)	11.7705(5)	311.38(5)
α-Sb_2O_4	5.4429(3)	4.8084(3)	11.7810(6)	308.33(3)

XDS2000 diffractometer at room temperature (Cu$K\alpha$ radiation, θ–θ mode, flat plate geometry) in the 2θ range 3°–110° with a step size of 0.02° and a step time of 10 s. The diffraction patterns were analyzed using the Rietveld method (25) with the FULLPROF program (26). The peaks were indexed on an orthorhombic cell, with refinement of the unit-cell constants for $SbSb_xM_{1-x}O_4$ (M = Nb or Ta; $x = 0.2$, 0.4, 0.5, 0.6, 0.8) performed using a least-squares method (see Table 1). The structural refinements of $SbSb_{0.5}M_{0.5}O_4$ (M = Nb or Ta) were carried out in the space group $Pna2_1$ (No. 33) with a starting model similar to $SbNbO_4$ (19). A total of 33 parameters, including 11 profile parameters, were used during the refinements. An asymmetry correction was applied to the low-angle reflections. The scale was refined initially, followed in subsequent iterations by the zero point error, cell constants, peak shape parameters, atomic parameters, and overall isotropic temperature factors. The results of the refinements are summarized in Table 2, with atomic positions and isotropic thermal parameters given in Table 3.

Second-order nonlinear optical measurements. Powder SHG measurements were performed on a modified Kurtz–NLO (27) system using 1064-nm light. A Continuum Minilite II laser, operating at 15 Hz, was used for all measurements. The average energy per pulse was 3 mJ. Since the SHG efficiency of powders has been shown to depend strongly on particle size (27, 28), polycrystalline α-Sb_2O_4, $SbNbO_4$, and $SbTaO_4$ were ground and sieved (Newark Wire Cloth Co.) into distinct particle size ranges: < 20 μm, 20–45 μm, 45–63 μm, 63–75 μm, 75–90 μm, and 90–125 μm. For the compounds in the solid solution, the powders in the 45–63 μm were used for SHG intensity measurements. To make relevant comparisons with known SHG materials, crystalline SiO_2 was also ground and sieved into the same particle size ranges. All the powders were placed in separate capillary tubes. The SHG, i.e., 532 nm green light, radiation was collected in reflection and detected by a photomultiplier tube (Oriel Instruments). To detect only the SHG light, a 532 nm narrow-bandpass interference filter was attached to the tube. A digital oscilloscope (Tektronix TDS 3032) was used to view the SHG signal.

TABLE 2
Summary of Crystallographic Data and Refinement Results for $Sb(Sb_{0.5}M_{0.5})O_4$ (M = Nb or Ta)

Compound	$Sb(Sb_{0.5}Nb_{0.5})O_4$	$Sb(Sb_{0.5}Ta_{0.5})O_4$
a (Å)	5.5140(2)	5.5019(2)
b (Å)	4.8761(2)	4.8762(2)
c (Å)	11.7961(5)	11.8038(4)
V (Å^3)	317.16(5)	316.68(5)
Space group	$Pna2_1$ (No. 33)	$Pna2_1$ (No. 33)
Observations	413	412
χ^2	2.30	2.24
R_p[a]	0.116	0.163
R_{wp}[b]	0.152	0.181
R_{exp}[c]	0.101	0.121
R_{Bragg}[d]	0.046	0.064

Note. I_o and I_c are the observed and calculated integrated intensities, I_k is the Bragg intensity, and w is the weight derived from an error propagation scheme during the process of least-squares refinement.

[a] $R_p = \sum |I_o - I_c| / \sum I_o$.

[b] $R_{wp} = [\sum w |I_o - I_c|^2 / \sum w I_o^2]^{1/2}$.

[c] $R_{exp} = R_{wp}/(\chi^2)^{1/2}$.

[d] $R_{Bragg} = \sum |I_{k(obs)} - I_{k(calc)}| / \sum I_{k(obs)}$.

TABLE 3
Fractional Atomic Coordinates, Isotropic Temperature Factors (Å^2), and Occupancies for $Sb(Sb_{0.5}M_{0.5})O_4$ (M = Nb or Ta)

Atom	x	y	z	B_{iso}	Occupancy
		$Sb(Sb_{0.5}Nb_{0.5})O_4$			
Nb/Sb(1)	0.1194(6)	− 0.006(2)	− 0.071(1)	1.7(1)	0.5/0.5[a]
Sb(2)	0.478(1)	0.043(6)	0.178(2)	2.1(1)	1.0
O(1)	0.183(6)	− 0.149(6)	− 0.226(3)	0.8(3)[b]	1.0
O(2)	0.420(6)	− 0.188(6)	− 0.008(3)	0.8(3)[b]	1.0
O(3)	0.146(6)	0.182(6)	0.087(3)	0.8(3)[b]	1.0
O(4)	0.363(6)	0.281(6)	− 0.123(3)	0.8(3)[b]	1.0
		$Sb(Sb_{0.5}Ta_{0.5})O_4$			
Ta/Sb(1)	0.1249(6)	− 0.005(3)	− 0.138(1)	2.2(1)	0.5/0.5[a]
Sb(2)	0.479(2)	0.045(1)	0.112(2)	3.0(2)	1.0
O(1)	0.154(9)	− 0.116(9)	− 0.327(3)	0.3(6)[c]	1.0
O(2)	0.353(9)	− 0.289(9)	− 0.084(3)	0.3(6)[c]	1.0
O(3)	0.159(9)	0.186(9)	− 0.002(3)	0.3(6)[c]	1.0
O(4)	0.424(9)	0.185(9)	− 0.188(3)	0.3(6)[c]	1.0

[a] Statistically disordered with 50% Sb^V and 50% M^V ($M = Nb^V$ or Ta^V). Atomic coordinates constrained to be equal.
[b,c] Thermal parameters constrained to be equal.

RESULTS AND DISCUSSION

Both $SbNbO_4$ and $SbTaO_4$ form solid solutions with α-Sb_2O_4. The powder X-ray diffraction data for both solid solutions are shown in Figs. 2a and 2b, with the refined unit cell for each compound given in Table 1. As expected, the cell volume decreases with increasing Sb^V on the Nb^V or Ta^V site. The volume change is less for the α-Sb_2O_4–$SbTaO_4$ solid solution than for α-Sb_2O_4–$SbNbO_4$. This is attributable to the similar size of six-coordinate Sb^V (0.60 Å) compared with that of six-coordinate Ta^V (0.64 Å), which is smaller than six-coordinate Nb^V (0.68 Å) (29). However, the unit cell changes are anisotropic, with the changes in a and b around 2%, whereas the change in c is only $\sim$0.25%. This anisotropic change in unit cell is consistent with the loss of polarization in changing from a M^VO_6 octahedra to Sb^VO_6 octahedra (vide infra). We were able to refine the structures for $SbSb_{0.5}Nb_{0.5}O_4$ and $SbSb_{0.5}Ta_{0.5}O_4$ (see Table 2 and auxiliary material).[2] We did not observe any ordering between Sb^V and M^V ($M = Nb^V$ or Ta^V) throughout the range of the solid solutions.

The SHG behaviour of the $SbSb_xM_{1-x}O_4$ ($M = Nb^V$ or Ta^V) solid solutions is shown in Figs. 3a and 3b. For both solid solutions the SHG efficiency decreases markedly for $x \geq 0.6$, i.e., $SbSb_{0.6}M_{0.4}O_4$, and for pure α-Sb_2O_4 the SHG is only slightly more efficient than SiO_2. *This would strongly*

[2] Experimental and calculated powder X-ray diffraction data and difference plots for $SbSb_{0.5}Nb_{0.5}O_4$, $SbSb_{0.5}Ta_{0.5}O_4$ and indexed powder X-ray diffraction data for $SbSb_xM_{1-x}O_4$ ($M = Nb^V$ or Ta^V) for $x = 0.0$, 0.2, 0.4, 0.6, 0.8, and 1.0 are available from the author upon request.

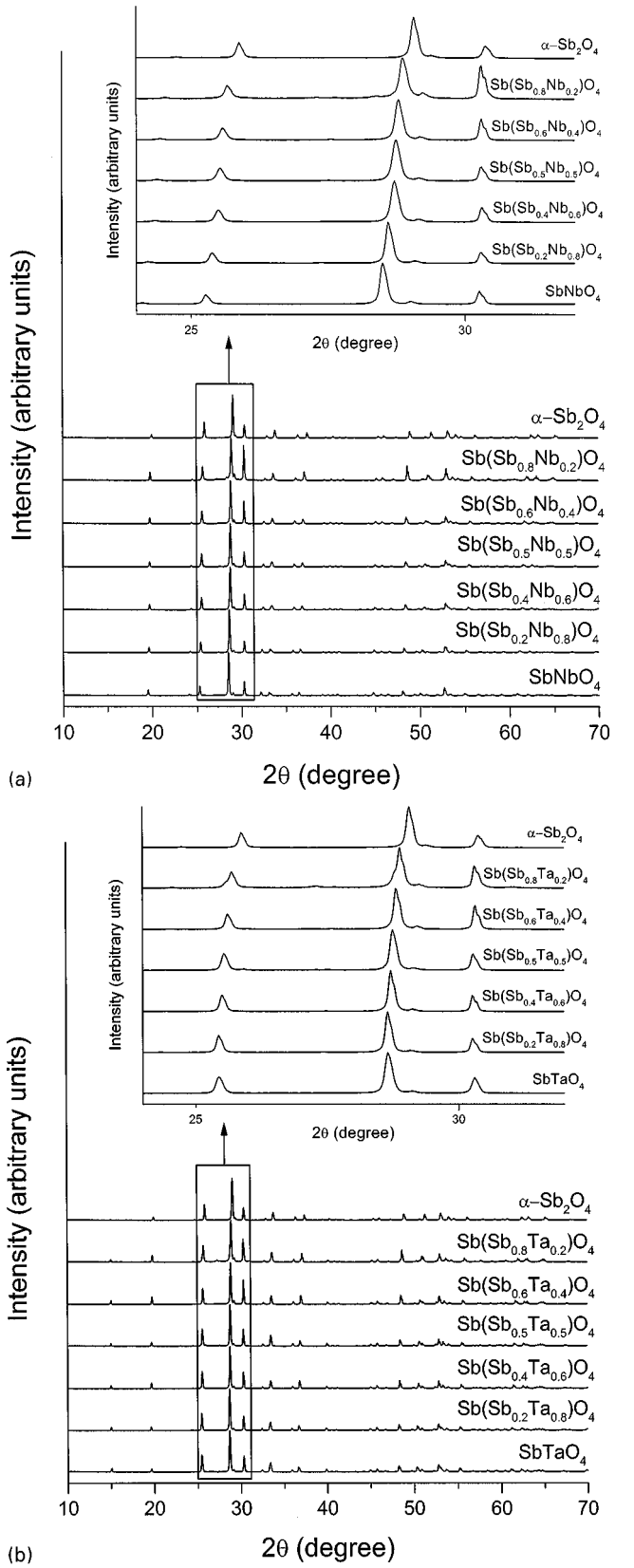

FIG. 2. Powder X-ray diffraction data for (a) $SbSb_xNb_{1-x}O_4$ and (b) $SbSb_xTa_{1-x}O_4$.

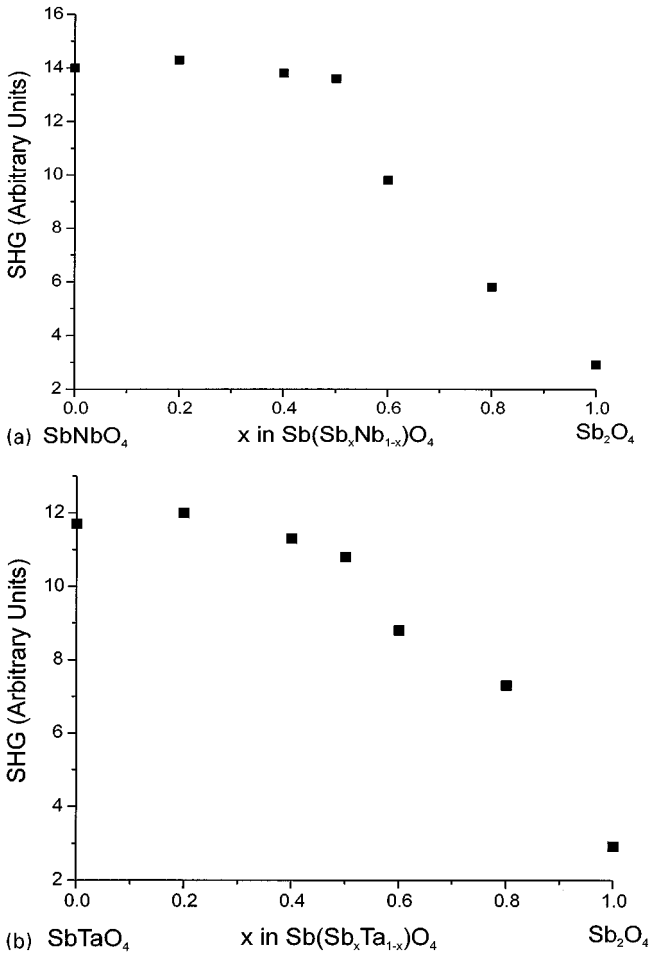

FIG. 3. SHG vs Sb^V doping in (a) $SbSb_xNb_{1-x}O_4$ and (b) $SbSb_xTa_{1-x}O_4$. In both figures, note the marked decrease in SHG efficiency for $x \geq 0.6$

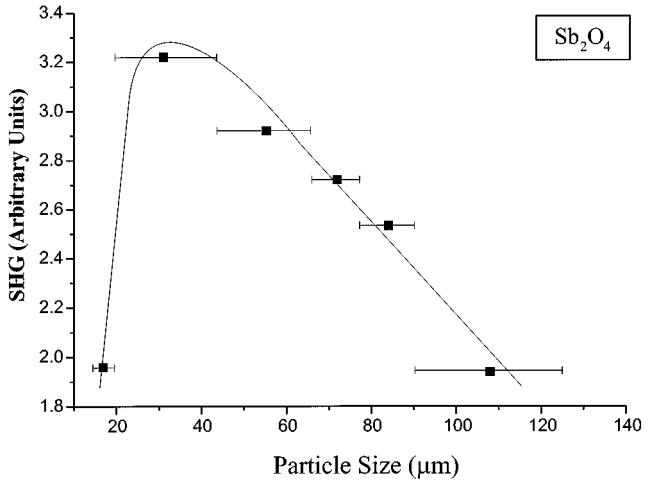

FIG. 4. Phase matching, i.e., particle size vs SHG intensity, data for α-Sb_2O_4. The curve is drawn to guide the eye and is not a fit to the data.

suggest that the structural origin of the SHG is attributable to the distorted MO_6 ($M = Nb^V$ or Ta^V) octahedra and not the $Sb^{III}O_4E$ group, even though both cations, M^V and Sb^{III}, are in asymmetric coordination environments. The reduction in SHG is consistent with the net polarization of the respective metal polyhedra. The Sb^{III} cation, in $SbMO_4$, is in an asymmetric coordination environment attributable to the nonbonded electron pair. The cation is bonded to four oxygen atoms in a distorted square pyramidal geometry. In the $SbMO_4$ structure, the polarization on the $Sb^{III}O_4E$ group alternates between the [010] and [0$\bar{1}$0] directions. Thus, the *net* polarization, i.e., dipole moment, associated with Sb^{III} in NCS $SbMO_4$ is zero. The M^V cations ($M = Nb^V$ or Ta^V) are also in a distorted coordination environment. Here, the cation is intraoctahedrally distorted, resulting in two "short" and four "long" bonds to oxygen. When the M^V octahedra are taken in their entirely, a *net* polarization, i.e., dipole moment, is observed along the [011] direction. Thus, from a structural approximation the SHG efficiency is attributable to this M^V polarization. When Sb^V is substituted for this "polarized" cation, the SHG efficiency decreases. This decrease is attributable to the isotropic environment of Sb^V, i.e., no dipole moment in the Sb^VO_6 octahedra. Thus, similar to replacing Ti^{IV} with Sn^{IV} in $KTiOPO_4$ (KTP) (30), the inclusion of a nonpolarizable cation, in our case Sb^V, is detrimental to the SHG efficiency.

As previously stated, the single-crystal NLO behavior of $SbNbO_4$ and $SbTaO_4$ has been studied (21, 31). We investigated the powder SHG behavior for α-Sb_2O_4, $SbNbO_4$, and $SbTaO_4$ and determined that none of the materials are phase matchable (see Figs. 4, 5, and 6). We also determined that the compounds have SHG efficiencies of 10, 400, and 350 times SiO_2, respectively. Previous SHG measurements on single-crystals $SbMO_4$ ($M = Nb^V$ or Ta^V) enabled the

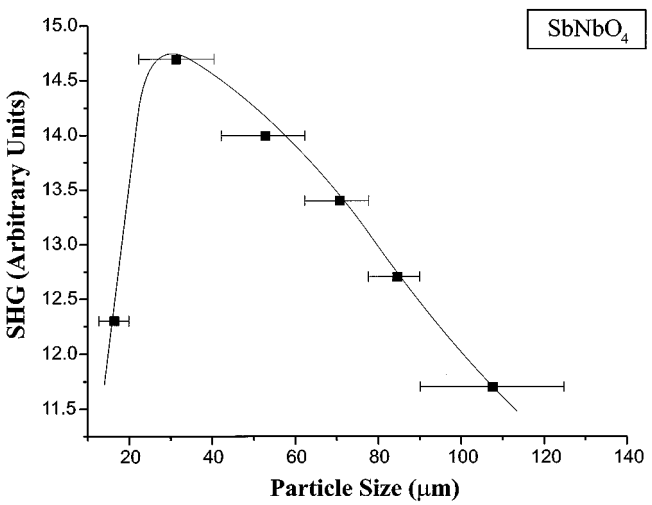

FIG. 5. Phase matching, i.e., particle size vs SHG intensity, data for $SbNbO_4$. The curve is drawn to guide the eye and is not a fit to the data.

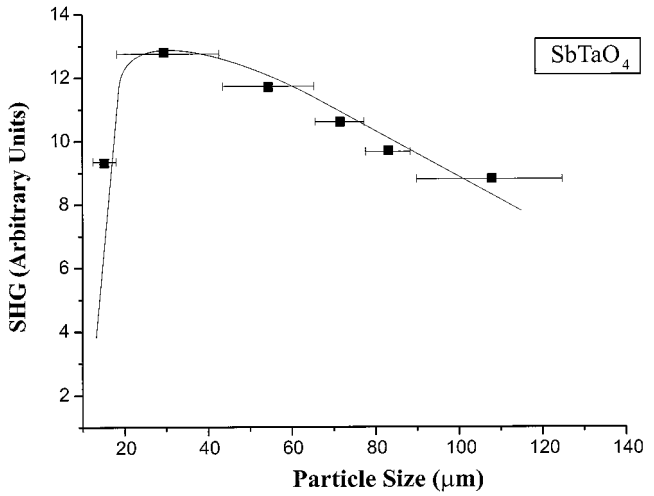

FIG. 6. Phase matching, i.e., particle size vs SHG intensity, data for $SbTaO_4$. The curve is drawn to guide the eye and is not a fit to the data.

researchers to deduce the specific $\langle d_{ijk}^{2\omega}\rangle$, NLO bond susceptibility, values. $SbNbO_4$ and $SbTaO_4$ crystallize in the orthorhombic space group $Pna2_1$, which is in point group $mm2$. Point group $mm2$ has three independent SHG modulii, assuming Kleinman symmetry is valid (32); $d_{311} = d_{113}$, $d_{322} = d_{223}$, and d_{333}. In their original paper, Kurtz and Perry deduced that for unpolarized fundamental and second-harmonic light (27)

$$(\langle d_{ijk}^{2\omega}\rangle)^2 = (19/105)\sum_i (d_{iii})^2 + (13/105)\sum_{i\neq j}(d_{iii})(d_{ijj}) + (44/105)\sum_{i\neq j}(d_{iij})^2 + (13/105)\sum_{ijk,\,\text{cyclic}}(d_{iij})(d_{jkk}) + (5/7)(d_{ijk})^2. \quad [1]$$

For point group, i.e., crystal class, $mm2$, Eq. [1] reduces to

$$(\langle d_{ijk}^{2\omega}\rangle)^2 = (19/105)(d_{333})^2 + (26/105)(d_{333})(d_{311}) + (44/105)(d_{113})^2 + (44/105)(d_{223})^2 + (26/105)(d_{113})(d_{223}). \quad [2]$$

For $SbNbO_4$, $d_{311} = 5.90$ pm/V and $d_{223} = 5.75$ pm/V (21, 31). Putting these values into Eq. [2],

$$\{(\langle d_{ijk}^{2\omega}\rangle)^2\,(SbNbO_4)\} = (0.18)(d_{333})^2 + 1.46\ \text{pm/V}\,(d_{333}) + 36.9\ \text{pm}^2/\text{V}^2. \quad [3]$$

For two non-phase-matchable materials, the intensity ratio can be written (27)

$$I^{2\omega}(SbNbO_4)/I^{2\omega}(SiO_2) = \left[(\langle d_{ijk}^{2\omega}\rangle)^2 \times \frac{(l_c)^2}{2r}\right](SbNbO_4)/\left[(\langle d_{ijk}^{2\omega}\rangle^2) \times \frac{(l_c)^2}{2r}\right](SiO_2). \quad [4]$$

TABLE 4
Summary of SHG Data

Compound	$I^{2\omega}/I^{2\omega}(SiO_2)$	$\langle d_{ijk}^{2\omega}\rangle$
SiO_2	1	0.28 pm/V[a]
α-Sb_2O_4	10	1.8 pm/V[b]
$SbNbO_4$	400	11.0 pm/V[b]
$SbTaO_4$	350	10.1 pm/V[b]
$SbSb_{0.5}Nb_{0.5}O_4$	375	10.7 pm/V[b]
$SbSb_{0.5}Ta_{0.5}O_4$	300	9.6 pm/V[b]
Approximate NLO bond susceptibilities		
d_{333} ($SbNbO_4$)	18 pm/V[b]	
d_{333} ($SbTaO_4$)	17 pm/V[b]	

[a] Calculated from reported single-crystal NLO data.
[b] This work.

The coherence length, l_c, is 20 μm for SiO_2 and is assumed to be 10 μm for $SbNbO_4$, whereas the average particle size, r, is taken to be 50 μm for both materials (27). The value of $\{(\langle d_{ijk}^{2\omega}\rangle)^2\,(SiO_2)\}$ can be calculated from single-crystal data and is equal to 7.62×10^{-2} pm^2/V^2. $SbNbO_4$ has an SHG intensity of 400 times SiO_2. Setting Eq. [4] equal to 400 and solving for $\{(\langle d_{ijk}^{2\omega}\rangle)^2\,(SbNbO_4)\}$ results in a value of 1.22×10^2 pm^2/V^2. Therefore, Eq. [3] becomes

$$1.22 \times 10^2\ \text{pm}^2/\text{V}^2 = (0.18)(d_{333})^2 + 1.46\ \text{pm/V}\,(d_{333}) + 36.9\ \text{pm}^2/\text{V}^2. \quad [5]$$

Solving Eq. [5] for d_{333} results in a value of approximately 18 pm/V. Repeating the procedure for $SbTaO_4$, which has a SHG efficiency of 350 times SiO_2 with $d_{311} = 5.10$ pm/V and $d_{223} = 5.00$ pm/V (21, 31), results in a $\{(\langle d_{ijk}^{2\omega}\rangle)^2\,(SbTaO_4)\}$ value of 1.07×10^{-2} pm^2/V^2. Thus, d_{333} for $SbTaO_4$ is approximately 17 pm/V.

Based only on powder SHG data, we may calculate the average bond susceptibility value, $\langle d_{ijk}^{2\omega}\rangle$, for α-Sb_2O_4, $SbSb_{0.5}Nb_{0.5}O_4$, and $SbSb_{0.5}Ta_{0.5}O_4$. These materials have a SHG efficiency of 10, 375, and 300 times SiO_2. Also all the materials are not phase matchable. Equation [4] describes the intensity ratio for two non-phase-matchable materials. This equation may be solved for $\langle d_{ijk}^{2\omega}\rangle$ for α-Sb_2O_4, $SbSb_{0.5}Nb_{0.5}O_4$, and $SbSb_{0.5}Ta_{0.5}O_4$, respectively, by setting Eq. [4] equal to 10, 375, and 300 and using the same values for l_c and r as before. Doing so results in values of 1.8, 10.7, and 9.6 pm/V for α-Sb_2O_4, $SbSb_{0.5}Nb_{0.5}O_4$, and $SbSb_{0.5}Ta_{0.5}O_4$, respectively. These values are the *average* NLO bond susceptibilities, for the entire material, and not for specific susceptibility tensors. Table 4 summarizes the SHG data described in this paper.

CONCLUSION

The solid solution and powder SHG behavior of α-Sb_2O_4–$SbNbO_4$ and α-Sb_2O_4–$SbTaO_4$ has been

investigated. We determined that both $SbNbO_4$ and $SbTaO_4$ form solid solutions with α-Sb_2O_4. We also determined that the SHG efficiency decreases markedly in $SbSb_xM_{1-x}O_4$ ($M = Nb^V$ or Ta^V) for $x \geq 0.6$. The decrease in SHG upon the addition of Sb^V strongly suggests that the structural origin for the SHG is attributable to the distorted M^VO_6 octahedra and not the $Sb^{III}O_4E$ group. This is consistent with the observation that the SHG efficiency of $SbNbO_4$ and $SbTaO_4$ are substantially greater than α-Sb_2O_4. We are in the process of investigating other SHG materials and will be reporting on them shortly.

ACKNOWLEDGMENTS

We thank the Robert A. Welch Foundation for support. This work used the MRSEC/TCSUH Shared Experimental Facilities supported by the National Science Foundation under Award DMR-9632667 and the Texas Center for Superconductivity at the University of Houston. This work was also supported by the NSF-Career Program through DMR-0092054.

REFERENCES

1. C. Chen and G. Liu, *Ann. Rev. Mater. Sci.* **16,** 203 (1986).
2. S. R. Marder, J. E. Sohn, and G. D. Stucky, *in* "Materials for Non-Linear Optics: Chemical Perspectives." Am. Chem. Soc. Washington, D.C., 1991.
3. P. S. Halasyamani and K. R. Poeppelmeier, *Chem. Mater.* **10,** 2753 (1998).
4. P. Becker, *Adv. Mater.* **10,** 979 (1998).
5. D. A. Keszler, *Curr. Opin. Solid State Mater. Sci.* **4,** 155–162 (1999).
6. J. F. Nye, "Physical Properties of Crystals." Oxford Univ. Press, Oxford, 1957.
7. U. Opik and M. H. L. Pryce, *Proc. R. Soc.* (*London*) *A* **238,** 425 (1957).
8. R. F. W. Bader, *Mol. Phys.* **3,** 137 (1960).
9. R. F. W. Bader, *Can. J. Chem.* **40,** 1164 (1962).
10. R. G. Pearson, *J. Am. Chem. Soc.* **91,** 4947 (1969).
11. R. G. Pearson, *J. Mol. Struct.* (*Theochem*) **103,** 25 (1983).
12. R. A. Wheeler, M.-H. Whangbo, T. Hughbanks, R. Hoffmann, J. K. Burdett, and T. A. Albright, *J. Am. Chem. Soc.* **108,** 2222 (1986).
13. M. Kunz and I. D. Brown, *J. Solid State Chem.* **115,** 395 (1995).
14. Y. Porter, N. S. P. Bhuvanesh, and P. S. Halasyamani, *Inorg. Chem.* **40,** 1172 (2001).
15. K. M. Ok, N. S. P. Bhuvanesh, and P. S. Halasyamani, *Inorg. Chem.* **40,** 1978 (2001).
16. Y. Porter, K. M. Ok, N. S. P. Bhuvanesh, and P. S. Halasyamani, *Chem. Mater.* **13,** 1910 (2001).
17. P. S. Gopalakrishnan and H. Manohar, *Cryst. Struct. Commun.* **4,** 203 (1975).
18. J. Amador, E. P. Gutierrez, M. A. Monge, I. Rasines, and C. R. Valero, *Inorg. Chem.* **27,** 1367 (1987).
19. A. N. Lobachev, V. F. Peskin, V. I. Popolitov, L. N. Syrkin, and N. N. Feoktistova, *Sov. Phys.-Solid State* **14,** 509 (1972).
20. V. I. Popolitov, A. N. Lobachev, V. F. Peskin, L. N. Syrkin, and N. N. Feoktistova, *Sov. Phys.-Crystallogr.* **18,** 258 (1973)
21. V. I. Popolitov, L. A. Ivanova, S. Y. Stephanovitch, V. V. Chetchkin, A. N. Lobachev, and Y. N. Venevtsev, *Ferroelectrics* **8,** 519 (1974).
22. W. Jeitschko and A. W. Sleight, *Acta Crystallogr. B* **30,** 2088 (1974).
23. R. S. Roth and J. L. Waring, *Am. Miner.* **48,** 1348 (1963).
24. A. C. Skapski and D. Rogers, *Chem. Commun.* 611 (1965).
25. H. M. Rietveld, *J. Appl. Crystallogr.* **2,** 65 (1969).
26. J. C. Rodriguez, "*FULLPROF Program*: *Rietveld Pattern Matching Analysis of Powder Patterns*," ILL Grenoble, 1990.
27. S. K. Kurtz and T. T. Perry, *J. Appl. Phys.* **39,** 3798 (1968).
28. J. P. Dougherty and S. K. Kurtz, *J. Appl. Crystallogr.* **9,** 145 (1976).
29. R. D. Shannon, *Acta Crystallogr. A* **32,** 751 (1976).
30. M. L. F. Phillips, W. T. A. Harrison, and G. D. Stucky, *Inorg. Chem.* **29,** 3245 (1990).
31. L. A. Ivanova, V. I. Popolitov, S. Y. Stefanovich, A. N. Lobachev, and Y. N. Venevtsev, *Sov. Phys.-Crystallogr.* **19,** 356 (1974).
32. D. A. Kleinman, *Phys. Rev.* **126,** 1977 (1962).